Review

Key enzymes in the anaerobic aromatic metabolism catalysing Birch-like reductions

Matthias Boll*

Institut für Biologie II, Universität Freiburg, Schänzlestr. 1, D-79104 Freiburg, Germany

Abstract

Several novel enzyme reactions have recently been discovered in the aromatic metabolism of anaerobic bacteria. Many of these reactions appear to be catalyzed by oxygen-sensitive enzymes by means of highly reactive radical intermediates. This contribution deals with two key reactions in this metabolism: the ATP-driven reductive dearomatisation of the benzene ring and the reductive removal of a phenolic hydroxyl group. The two reactions catalyzed by benzoyl-CoA reductase (BCR) and 4-hydroxybenzoyl-CoA reductase (4-HBCR) are both mechanistically difficult to achieve; both are considered to proceed in 'Birch-like' reductions involving single electron and proton transfer steps to the aromatic ring. The problem of both reactions is the extremely high redox barrier for the first electron transfer to the substrate (e.g., −1.9 V in case of a benzoyl-CoA (BCoA) analogue), which is solved in the two enzymes in different manners. Studying these enzymatic reactions provides insights into general principles of how oxygen-dependent reactions are replaced by alternative processes under anoxic conditions.
© 2004 Elsevier B.V. All rights reserved.

Keywords: Enzyme; Anaerobic; Birch-like

1. Introduction

Next to carbohydrates, aromatic compounds represent the second most abundant class of organic compounds in nature and therefore serve as important growth substrates for aerobic and anaerobic microorganisms. The relative resistance of aromatic compounds to biomineralization is due to the great stability caused by the resonance energy of the aromatic ring (>100 kJ mol^{-1}). The metabolism of aromatic compounds has long been considered to depend strictly on molecular oxygen for ring hydroxylation and ring cleavage reactions (for review, see Ref. [1]). In anaerobic bacteria, all enzymatic processes of the aromatic metabolism involving molecular oxygen are replaced by alternative reactions. In recent years, several novel biochemical processes were discovered and characterised in the anaerobic aromatic metabolism (for recent reviews see, Refs. [2–5]): (i) the reductive dearomatisation of the aromatic ring, (ii) the reductive removal of functionalities at the aromatic ring (e.g., the reductive dehydroxylation, dehalogenation, etc.), (iii) the carboxylation/decarboxylation of the aromatic ring (e.g., phenol carboxylation), (iv) several oxidations without oxygen as co-substrate (e.g., oxidation of the alkyl functionalities of toluene or ethylbenzene, hydroxylation of the aromatic ring, transhydroxylation reactions). This review addresses itself to enzymes catalysing unusual reductions of type (i) and (ii) which both require coenzyme A thiol esters as substrates.

The strategy of anaerobic bacteria is to convert the multitude of low-molecular weight aromatic growth substrates into only a few key intermediates, which are substrates for the corresponding dearomatising reductases; these are benzoyl-CoA (BCoA), phloroglucinol, hydroxyhydroquinone and resorcinol (Refs. [2–5], Fig. 1). The
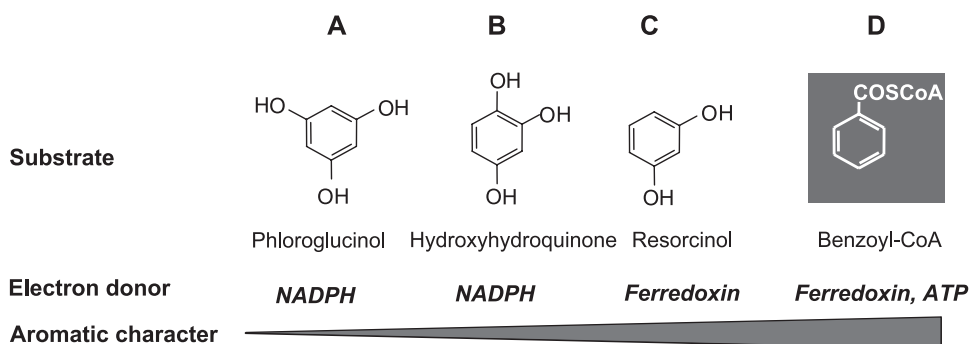
Fig. 1. Substrates and electron donors for dearomatising enzymes in the aromatic metabolism of anaerobic bacteria. The substrates for the following enzymes are lined up according to their increasing aromatic character: (A) Phloroglucinol reductase, (B) *para*-hydroxyhydroquinone reductase, (C) resorcinol reductase, and (D) BCR.

latter three compounds all contain *meta*-positioned hydroxyl-groups which largely weaken the aromatic character. As a consequence, the two-electron reductions of these compounds can be accomplished in exergonic reactions with common physiological reductants. NAD(P)H (in case of phloroglucinol and hydroxyhydroquinone [6,7]) or ferredoxin (in case of resorcinol [8]) serve as electron donors for the corresponding reductases. In contrast, due to the fully developed aromatic character of the benzene ring, BCoA is difficult to reduce by a physiological reductant. The only enzyme known so far which is able to reduce BCoA uses not only the low-potential electron donor ferredoxin but, in addition, couples ring reduction to a stoichiometric hydrolysis of ATP [9,10]. The biochemistry of Benzoyl-CoA reductase (dearomatising, BCR) has solely been studied in one organism so far, in the denitrifying facultative anaerobic bacterium *Thauera aromatica*.

The reductive removal of functionalities from the benzene nucleus represents a second enzymatic process which is characteristic in the anaerobic aromatic metabolism. So far, the few examples for this process studied are the reductive dehalogenation, deamination and dehydroxylation. In each case, benzoate derivatives are the substrates for the corresponding reductases [3,4]. Among these reactions, the reductive dehydroxylation plays an important role in nature as most biogenic benzoic acid derivatives contain phenolic hydroxyl functionalities (e.g., phenylpropanes, flavonoids, salicylic acid, tannins, etc.). So far, 4-hydroxybenzoyl-CoA reductase (dehydroxylating, 4-HBCR) from the denitrifying bacterium *T. aromatica* represents the best characterised enzyme catalysing the reductive removal of a functionality from the benzene ring [11,12].

In this review, the physiology, molecular biology and biochemistry of BCR and 4-HBCR will be discussed and compared. The reactions catalyzed by both enzymes are considered to proceed in similar mechanisms by means of extremely reactive radical intermediates. The focus of this contribution addresses the question how enzymes with a totally different composition solve similar energetic and mechanistic problems posed by the reaction catalyzed.

2. BCR and 4-HBCR: two different enzymes catalysing Birch-like reductions?

In organic synthesis up to the industrial scale, aromatic ring reductions are usually performed in a so-called Birch reduction. The mechanism of this process includes alternate single electron and proton transfer steps to the benzene ring, which result in the reductive dearomatisation of the benzene nucleus or in the dehydroxylation of phenols; the latter are subsequently further reduced [13,14]. The rate-limiting step of this mechanism is the first electron transfer step yielding a radical anion, which has an extremely low redox potential (e.g., − 3 V for non-substituted benzene [15]). To overcome this high redox barrier, solvated electrons, the most potent reductants known in organic chemistry, are used in Birch reductions. These are usually generated by dissolving alkali metals in liquid ammonia; a very weak proton donor (usually an alcohol) is used to avoid H^+ reduction to H_2. The subsequent protonation of the radical anion to the neutral radical pulls the reaction forwards. Note that the transfer of the second electron to the neutral radical is thermodynamically much more favoured than the first one (Fig. 2).

Considering the harsh and unphysiological conditions of Birch reductions, it was surprising to discover enzymes catalysing similar reactions. Notably, both benzoate and 4-hydroxybenzoate are converted first into the corresponding coenzyme A thiol esters by specific ATP-dependent synthetases [16,17]. This thioesterification is considered as necessary activation step facilitating the following reduction processes catalysed by both reductases. Buckel and Keese [18] suggested a novel role for the coenzyme A thiol ester functionality in both the enzymatic dearomatisation of the aromatic ring and the dehydroxylation of phenolic compounds. They proposed that the carbonyl moiety of BCoA and 4-hydroxybenzoyl-CoA (4-HBCoA) essentially stabilises a ketyl radical anion intermediate, which is much easier to achieve than with non-substituted benzoic acid. The sequence of electron transfer and protonation steps in the proposed Birch reductions of BCoA and 4-HBCoA is depicted in Fig. 2. The redox potential
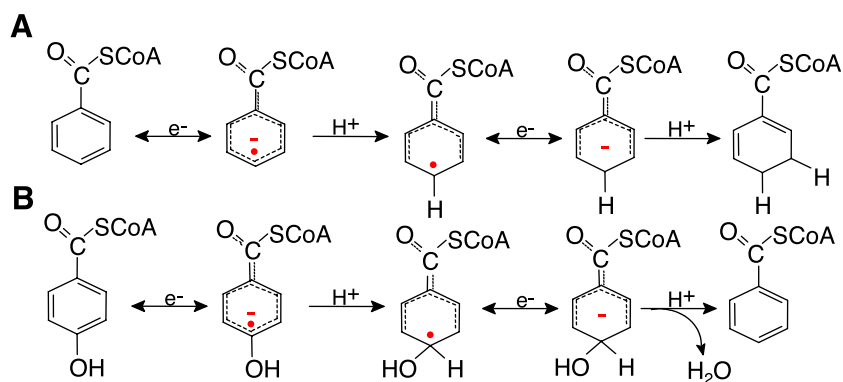
Fig. 2. Proposed 'Birch-like' mechanisms in enzymatic reductive dearomatisation of BCoA (A) and dehydroxylation of 4-HBCoA (B). The rate-limiting step in both reactions is the first electron transfer yielding a radical anion. The carbonyl oxygen largely contributes to the stabilisation of the radical intermediates.

determined for the one-electron transfer to the BCoA analogue, S-ethyl benzoic acid thiol ester (-1.9 V), is approximately 1 V more positive compared to benzoic acid [19]. However, still such a potential can hardly be achieved under physiological conditions. Therefore, catalysis by both reductases should involve a facilitated electron transfer to the aromatic ring, either by reducing the redox potential gap between the electron donor and the aromatic ring (e.g. by stabilisation of the radical intermediate) or by lowering the potential of electrons to be transferred to the aromatic ring (e.g., by coupling electron transfer to an exergonic process).

In spite of the proposed similar mechanisms, BCR and 4-HBCR have a totally different subunit architecture/cofactor composition (see below). Thus, the problem as to how highly reactive radical intermediates are stabilised appears to be solved in a different manner. Notably, enzymatic benzene ring reduction, but not the dehydroxylation of a phenolic hydroxyl group, is coupled to ATP-hydrolysis although the free energy of both overall reactions (using the low potential electron donor ferredoxin) appears to be negative or near thermodynamic equilibrium (exact ΔG-values for the thiol esters derivatives are not available).

3. BCR (dearomatising)

3.1. General properties of BCR from T. aromatica

BCR from *T. aromatica* catalyzes the ATP-driven transfer of two electrons from reduced ferredoxin to BCoA yielding cyclohexa-1,5-diene-1-carbonyl-CoA [19] (Fig. 3C). The identification of this thermodynamically favoured product confirmed earlier studies with cell extracts [20]. The formation of the conjugated 1,5-diene is in contrast to the classical Birch reduction in which the non-conjugated 2,5-diene represents the kinetically preferred product of the reduction of benzoic acid. BCR also catalyzes the ATP-dependent reduction of the non-physiological substrate hydroxylamine [9].

BCR reduces a number of BCoA analogues with F-, Cl-, OH-, NH_2, or CH_3- functionalities in *ortho*- and *meta*-positions at considerable rates [9,21] (see also Fig. 7). In case of 2-aminobenzoyl-CoA [22] and 3-hydroxybenzoyl-CoA [23], these reductions play a physiological role in the metabolism of the corresponding carboxylic acids. It is unknown whether the same holds true for the reduction of the other BCoA analogues.

BCR from *T. aromatica* hydrolyses two ATP to ADP and Pi for the two electrons transferred to the aromatic ring [24]. The low turnover number (4.8 s^{-1}) reflects the difficulty of the catalyzed reaction. The 170-kDa enzyme is a heterotetramer and consists of four subunits, with 49 (A), 48 (B), 44 (C) and 30 kDa (D) resulting in an ABCD composition (Fig. 3B). Metal analysis as well as EPR- and Mössbauer spectroscopic studies (see below) revealed three-cysteine-coordinated [4Fe-4S]$^{+1/+2}$ clusters [24,25]. The presence of a flavin cofactor, as suggested in an earlier study, can be ruled out [10]. Binding studies showed that the ATP binding sites of BCR allow some unspecific binding of compounds containing an adenosine nucleotide moiety such as coenzyme A or FAD (Möbitz and Boll, unpublished data). The genes coding for the four subunits are located in a gene cluster (*bad*-cluster; *b*enzoic *a*cid *d*egradation; Fig. 3A) [26]. This cluster in addition contains genes coding for the electron donor for BCR, ferredoxin, the ferredoxin reducing enzyme 2-oxoglutarate:ferredoxin oxidoreductase [26,27], and for further enzymes involved in BCoA metabolism. The following steps are catalyzed by the latter enzymes: the product of BCR, the conjugated 1,5-diene, is hydrated to a hydroxy monoene [28] which becomes oxidised to the corresponding ketone [29]. The second water addition to the remaining double bond and the subsequent hydrolytic cleavage of the ring are catalyzed by the same enzyme, 2-oxo-6-hydroxy-1-carbonyl-CoA hydrolase [29]. The formed aliphatic thiol ester, 3-hydroxypimelyl-CoA, is oxidised to three acetyl-CoA units and one CO_2 by a modified β-oxidation via glutaryl-CoA and crotonyl-CoA [30].
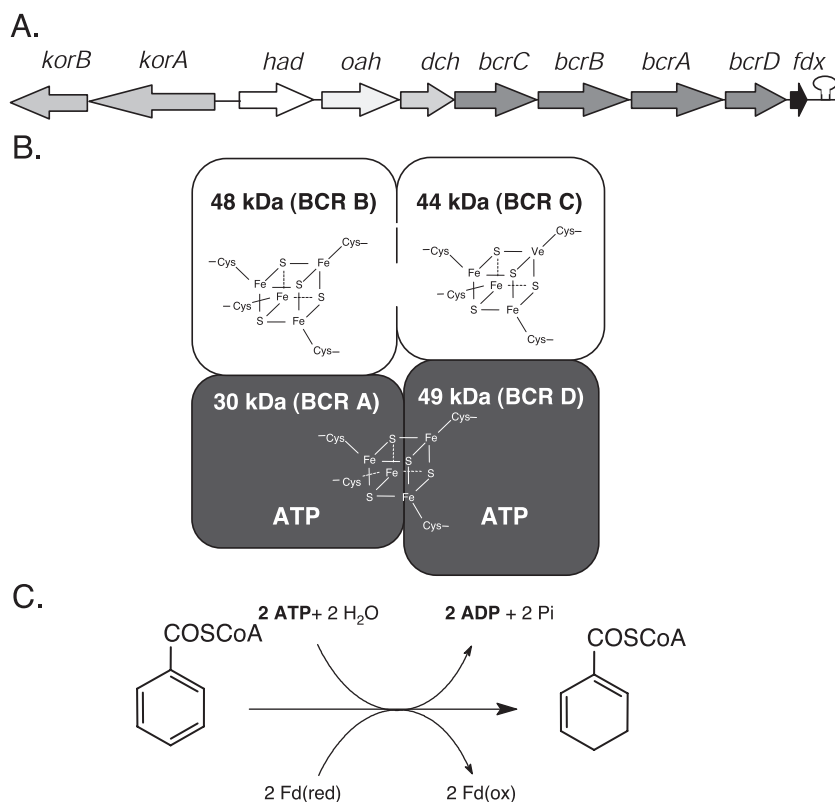
Fig. 3. Properties of BCR from *T. aromatica*: genes, architecture and reaction catalyzed. (A) The benzoic acid degradation gene cluster of *T. aromatica*. *bcrA*–*D* code for the four structural genes of BCR, *fdx* (ferredoxin) and *korA* and *B* (2-oxoglutarate:ferredoxin oxidoreductase) for proteins involved in electron transfer to BCoA. The other genes code for enzymes involved in oxidation/ring opening reactions: *dch*, cyclohexa-1,5-diene-1-carbonyl-CoA hydratase; *had*, 6-hydroxycyclohex-1-ene-1-carbonyl-CoA dehydrogenase; *oah*, ring opening hydrolase (3-oxo-acyl-CoA hydrolase). (B) Subunit/cofactor architecture of BCR. Subunits belonging to the same functional module are depicted in the same grey scale. (C) Reaction catalyzed by BCR.

Amino acid sequence comparisons with similar enzymes [26] (see Section 3.3) and spectroscopic studies [24,25] (see Section 3.4) indicate that BCR is composed of two structurally and functionally distinct modules: (i) the A and D subunits together form the site where electrons donated from reduced ferredoxin become activated by ATP hydrolysis. A single $[4Fe-4S]^{+1/+2}$ cluster, considered as primary electron acceptor, is coordinated by two conserved cysteines of the A- and D-subunits, respectively, resulting in an architecture resembling the nitrogenase Fe-protein (Fig. 3). The A- and D-subunits each contain one ATP-binding site of the ASKHA family [31,32] (acetate and sugar kinase, hsp70 and actin) differing from the Walker motifs involved in ATP binding of the nitrogenase Fe-protein [33]. Notably, there are significant amino acid sequence similarities between the A- and D-subunits (>20% in several regions), especially in the region containing the two ATP binding motifs. In spite of these similarities, both subunits largely differ in size resulting in an asymmetric assembly of this module. (ii) The B and C subunits are considered to form the reductase module, the site where the dearomatisation process takes place. Both subunits together contain 15 cysteine residues of which eight are supposed to coordinate two additional $[4Fe-4S]^{+1/+2}$ clusters. The BCoA binding site is also expected

to be located in this module although no typical coenzyme A binding motif could be identified (Möbitz and Boll, unpublished results).

3.2. BCR in other organisms

The number of identified facultative and obligate anaerobic bacteria metabolising low molecular aromatics is continuously increasing. The concept of the reductive dearomatisation as a key process in the anaerobic aromatic metabolism was originally postulated based on studies with the phototrophic *Rhodopseudomonas palustris* growing anaerobically in the light on benzoate as sole carbon source [34]. This organism was also the first, of which the genes coding for enzymes in the anaerobic benzoate metabolism were identified (*bad*-cluster, including the four structural genes of BCR [35]). Amino acid sequence comparisons of the four subunits of BCR from *R. palustris* (α-group of Proteobacteria) and *T. aromatica* (β-group of Proteobacteria) revealed high similarities in all four subunits (Table 1) including the size of subunits and conserved cysteines.

The genes putatively coding for the structural subunits of BCR have been identified in two further organisms. A cluster of genes similar to the *bad*-cluster in *T. aromatica*

Table 1
Similarities of the four subunits of BCR from *Thauera aromatica* (A–D) with other deduced proteins

Organism	Subunits/components			
	A	D	C	B
Thauera aromatica	100% CAA12249	100% CAA12250	100% CAA12247	100% CAA12248
Rhodopseudomonas palustris	69% AAC23927	70% AAC23928	64% AAC23925	76% AAC23926
*Magnetospirillum magnetotacticum*ZP 00053824	74% ZP 00053825	62% ZP 00053822	76% ZP 00053823	76% ZP 00053823
Azoarcus evansii	44% CAD21631	33% CAD21630	25% CAD21628	22% CAD21629
Desulfitobacterium hafniensii up	44% ZP 00098904	35%	27% ZP 00098906	29% ZP 00099739
Acidaminococcus fermentans Hgd	42% CAA42196	30%	24% CAA32466	25% CAA32465
Clostridium symbiosum Hgd	42% AAD31675	31%	23% AAD31677	24% AAD31676
Clostridium sporogenes Pld	42% AAL18809	31%	25% AAL18811	25% AAL18810

The values represent percentage amino acid sequence identity; the accession number is shown to the right; up, unknown protein; Hgd, hydroxyglutaryl-CoA dehydratase; Pld, phenyllactate dehydratase. Note that the dehydratases are two-component systems; the electron activating enzyme of this system (with similarities to the A and D subunits of BCR) is a homodimer.

and *R. palustris* was identified in the denitrifying *Azoarcus evansii* (β-group of Proteobacteria), which utilises a number of aromatic compounds. However, the amino acid sequence similarities of the four subunits of BCR from *A. evansii* with those of *T. aromatica* and *R. palustris* are significantly lower (Table 1); e.g., only 5 out of 15 cysteines are conserved in the B and C subunits between the enzymes from *A. evansii* and the other two organisms. In addition, the molecular mass of the putative A-subunit of BCR from *A. evansii* (∼ 30 kDa) largely differs from the corresponding subunits from *T. aromatica* and *R. palustris* (49 and 48 kDa, respectively). The genome of the magnetotactic *Magnetospirillum magnetotacticum* (α-group of Proteobacteria) contains four clustered open reading frames with very high similarities to the four subunits of BCR from *T. aromatica* and *R. palustris* (Table 1). Obviously, such genes appear to be distributed in distinct clusters in the α- and β-group of Proteobacteria. Nothing is known about the distribution of BCR in strictly anaerobic bacteria using aromatics as sole source of cell carbon and energy. For energetic reasons, it is questionable whether strict anaerobes can afford the coupling of benzene ring reduction to a stoichiometric ATP hydrolysis [4,9]. Therefore, a totally different enzymology might be involved in the dearomatisation of the aromatic ring in strictly anaerobic bacteria.

3.3. Similarities of BCR with other enzymes

BCR and nitrogenase exhibit several analogies including the coupling of ATP hydrolysis to the reduction of a chemically inert substrate and the similar architecture of the Fe-protein of nitrogenase and the electron activation module of BCR [36]. However, these analogies are not reflected in any amino acid sequence or cofactor similarities.

The amino acid sequences of the four subunits of BCR show significant similarities to enzymes which at first sight seem to catalyse a totally different reaction. In amino acid fermenting clostridia α-hydroxyacyl-CoA-dehydratases catalyse the mechanistically difficult dehydration of α-hydroxy thiol esters, which cannot be accomplished by one of the usual water elimination reactions as the β-hydrogen atom is not activated [37,38]. Thus, a different mechanism has been postulated involving radical intermediates whose formation requires electrons of an extremely low potential. Buckel and Keese [18] suggested that both the dearomatisation of the aromatic ring of BCoA and the dehydration of α-hydroxy acid thiol esters proceed via similar mechanisms (Fig. 4) [18]. In both cases, the formation of a ketyl radical anion intermediate is proposed to play a crucial role, which is largely facilitated by the thiol ester functionality of the substrate. Typical α-hydroxyacyl-CoA dehydratases are composed of two components: a heterodimeric dehydratase and a homodimeric electron activating enzyme. The latter activase couples the transfer of a single electron to the dehydratase component to a stoichiometric ATP hydrolysis. The activated electron is further transferred by the dehydratase to the substrate forming a ketyl radical anion. The subsequent elimination of water from the reactive radical intermediate is now more easily achieved than with the neutral molecule. Note that in contrast to BCoA reduction, the overall dehydration process is redox neutral. Therefore, the ATP-dependent electron activation has only a catalytic function in the dehydratase reaction as the low potential electron is assumed to stay on the enzyme for many catalytic cycles (Fig. 4).

The A- and D-subunits of BCR from *T. aromatica* show amino acid similarities to the single subunit of homodimeric electron activating enzymes from several amino acid fermenting clostridia (Table 1) [26,39]. In addition, the B- and C-subunits of BCR show similarities to the individual subunits of the actual heterodimeric dehydratases (e.g., 2-hydroxyglutaryl-CoA dehydratase from *Acidaminococcus fermentans* and other clostridia [40]). Recently, the crystal structure of the activase from *A. fermentans* confirmed the proposed molecular architecture of the activase from 2-hydroxyglutaryl-CoA dehydratase and the electron activation module of BCR from *T. aromatica* [41]. In some dehydratase components, a significant amount of molybdenum was found [42,43]. As no usual pterin cofactor
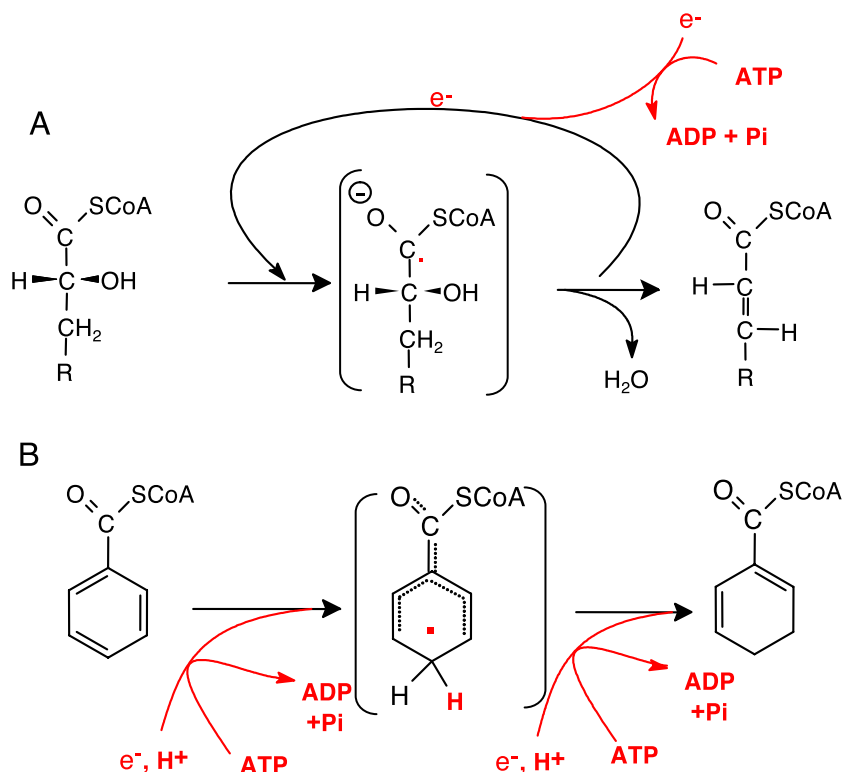
Fig. 4. Comparison of the simplified catalytic cycles of 2-hydroxyglutaryl-CoA dehydrates/activase (A) with BCR (B). Note that ATP-dependent electron activation in (A) is only catalytically required. Once the electron is activated, it stays on the enzyme for many cycles [37,38]. In BCR the first electron transfer is assumed to be assisted by simultaneous protonation yielding the free radical.

could be identified so far, it is assumed that some 2-hydroxyacyl-CoA dehydratases may represent a novel type of molybdenum enzymes.

3.4. Mechanism of electron transfer driven by ATP hydrolysis

The coupling of electron transfer to a stoichiometric ATP hydrolysis is a common property of BCRs, nitrogenases, and, though only catalytically relevant, of the electron activase component of α-hydroxyacyl-CoA dehydratases. In the following, the results providing insights into the ATP-dependent electron activation in BCR catalysis are summarised.

3.4.1. Binding of nucleotides

A recent kinetic study revealed that both ATP-binding sites of BCR are occupied sequentially [44]. The pre-steady state binding constants of the two ATP binding sites differ, which can be rationalised by the asymmetric design of the electron activation module (see Fig. 3B). Binding of a single nucleotide induces a 'nucleotide-binding switch' which is distinguished from the 'nucleotide-hydrolysis switch' (see below). As one major result of the former switch, BCR is converted from a closed to an open state. Only in this conformation BCoA is specifically bound; in parallel, the reduction rate of oxidised enzyme is clearly diminished [44].

3.4.2. ATPase activity

Evidence for a coupling of electron transfer and ATP hydrolysis is derived from studies of the ATP hydrolysing (ATPase) activity in the absence of a reducible substrate [24]. This futile activity is 15% of the normal rate coupled to substrate reduction. It is only observed in the dithionite-reduced state of the enzyme and can be simply switched off/on by mild oxidation/re-reduction of the enzyme. This finding indicated a strong coupling of the ATPase activity with the redox state of BCR, independent of the presence of BCoA.

3.4.3. S=7/2 high-spin state of a $[4Fe-4S]^{+1}$ cluster

The redox-state-dependent ATPase activity was further characterised by EPR and Mössbauer spectroscopy. Independent of the presence of the substrates MgATP and BCoA, the enzyme could be maximally reduced by one electron, even with excess of dithionite or deazaflavin/light as electron donors [24,25]. Typical EPR spectra of one-electron reduced BCR do not display a single fully reduced $[4Fe-4S]^{+1}$ cluster (out of three clusters in total) but rather two partially reduced species (Fig. 5A). Even more complicated, a portion of both partially reduced clusters interact magnetically, indicating that reduced BCR 'as isolated' consists of a mixture of species [24,25] (Fig. 5B). Addition of MgATP to reduced BCR (thereby initiating the ATPase activity) caused two effects resulting from ATP dependent
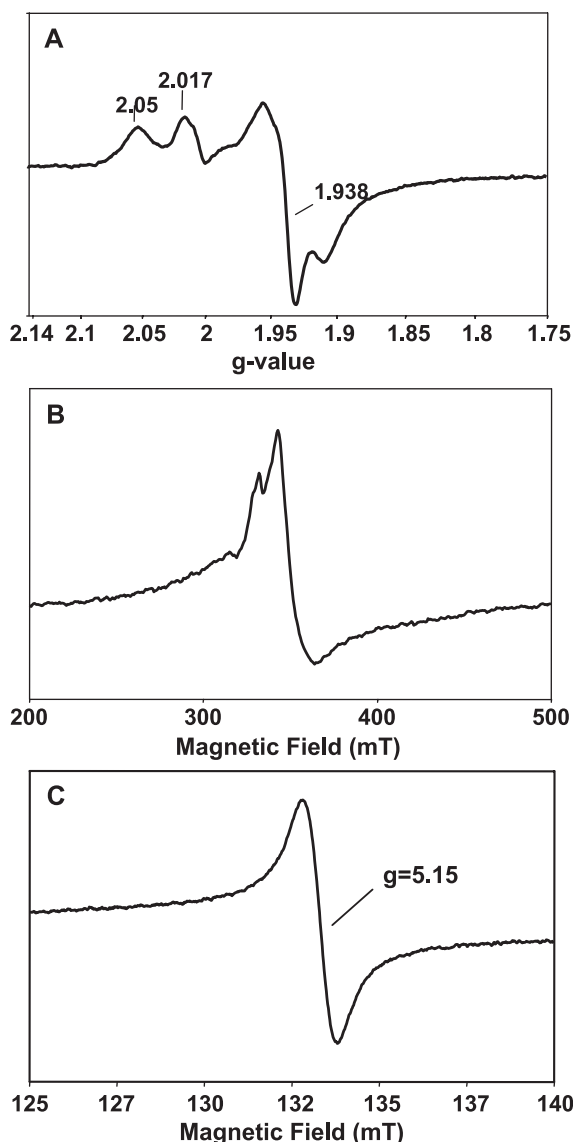
Fig. 5. Representative EPR spectra of dithionite reduced BCR. (A) Spectrum showing two non-interacting $[4Fe-4S]^+$ clusters recorded at 20 K and 2 mW microwave power. The numbers refer to representative *g*-values of two different $[4Fe-4S]^+$ clusters. (B) Spectrum showing two magnetically interacting $[4Fe-4S]^+$ clusters recorded at 4 K and 2 mW. (C) Spectrum showing the S = 7/2 high-spin state of a $[4Fe-4S]^+$ cluster recorded after addition of 10 mM MgATP and incubation at room temperature for 0.5 min; EPR-parameters are 25 K and 2 mW microwave power.

conformational changes: (i) the magnetic interaction of the two partially reduced clusters was diminished, and (ii) one cluster switched from the usual S = 1/2 low-spin to the S = 7/2 high-spin state [24,25]. The latter effect can be easily followed by EPR spectroscopy through the rise of a highly isotropic signal at $g = 5.15$, which represents the first excited state transition (S = ± 3/2) of an S = 7/2 high spin system (Fig. 5C). It is not clear which of the $[4Fe-4S]^{+1/+2}$ clusters of BCR undergoes the switch to the high-spin state. In the steady state of BCoA-independent ATPase activity, the high-spin state accounted for approximately 10% of a single

reduced $[4Fe-4S]^{+1}$ cluster; this proportion was sufficient to be detected by Mössbauer spectroscopy [25].

The S = 7/2 high-spin state is very unusual for protein coordinated $[4Fe-4S]^{+1}$ clusters and has so far only been observed in two other examples: in Se-substituted $[4Fe-4Se]^{+1/+2}$ clusters of ferredoxins [45] and in thionine oxidised P-cluster of nitrogenase from *Azotobacter vinelandii* [46]. However, both examples are considered as artificially generated species. In contrast, in single turnover experiments of BCR, the S = 1/2/S = 7/2 transition and the reverse switch back to the low-spin state were followed time-dependently, indicating that this transition represents a crucial event in catalysis.

The question arises: how can the switch to the S = 7/2 state be assigned to the activation of an electron driven by ATP hydrolysis? The formation of the S = 7/2 high-spin state should reflect conformational alterations in the vicinity of a $[4Fe-4S]^{+1/+2}$ cluster. As a result, the switched protein stabilises the S = 7/2 rather than the usual S = 1/2 state without the occurrence of intermediate spin states. It is established that in $[4Fe-4S]^+$ clusters, all iron atoms are high-spin [47]. For an S = 7/2 system, the three Fe^{2+} atoms couple ferromagnetically (S = 3 × 4/2 = 12/2), whereas the single high-spin Fe^{3+} atom (S = 1 × 5/2) couples antiferromagnetically giving the observed spin state of S = 12/2 − 5/2 = 7/2. The energy required for a S = 1/2/S = 7/2 switch was calculated in a theoretical approach using the FORTRAN program taking into account the estimated double and super exchange parameters [48]. The obtained value of − 40 to − 50 kJ mol^{-1} is in the range of the energy provided by hydrolysis of MgATP to MgADP and Pi under cellular conditions (~ 50 kJ mol^{-1}). With $\Delta E'\,° = - \Delta G'\,°/n \times F$, this value maximally accounts for a lowering of the redox potential by approximately 400–500 mV for the switched S = 7/2 cluster. In conclusion, the S = 7/2 state represents the activated state of a $[4Fe-4S]^{+1/+2}$ cluster in terms of a clearly lowered redox potential. The electrons donated from the natural donor reduced ferredoxin have a midpoint potential of ~ − 500 mV (average midpoint potential of both $[4Fe-4S]^{+1/+2}$ clusters of ferredoxin) [49], which is also in the range of the primary electron accepting $[4Fe-4S]^{+1/+2}$ cluster of BCR [25]. In conclusion, hydrolysis of one ATP per single electron could maximally lower the redox potential down to − 1.0 V (see also Fig. 9). Unfortunately, a direct determination of the MgATP dependent change in redox potential of a $[4Fe-4S]^{+1/+2}$ cluster is not possible as the activated electron continuously switches back from the activated S = 7/2 to the S = 1/2 ground state during the ATPase activity.

Two electrons have to be transferred to the aromatic ring for completing BCoA reduction to the corresponding diene. Therefore, the S = 1/2/S = 7/2 switch may occur twice per catalytic cycle. Alternatively, the energetically more demanding first electron transfer to the aromatic ring could be coupled to the hydrolysis of two ATP, whereas the second electron could be transferred without the input of

energy. Results from kinetic stopped-flow UV/VIS spectroscopic studies seem to rule out this alternative [44].

3.4.4. Kinase and autophosphatase activities

Independent of the redox state, BCR catalyses an isotope exchange from [14C]-labelled ADP to unlabeled ATP, suggesting that during catalysis a phosphorylated enzyme intermediate is formed [50]. The isotope exchange activity reflects a reversible, partial kinase partial activity of BCR:

$$ATP + E \rightleftharpoons ADP + E - P \tag{1}$$

$$E - P + [^{14}C]ADP \rightleftharpoons E + [^{14}C]ATP \tag{2}$$

In accordance with this activity, incubation with [γ-32P]-ATP resulted in the labelling of the C-subunit of BCR (44 kDa). Reduced but not oxidised BCR also catalyzed the autodephosphorylation of the formed enzyme-phosphate (phosphatase partial activity). This finding is in full accordance with the previous observation that only reduced BCR exhibits ATPase activity (see above) and demonstrates that the presence or absence of electrons governs partial (phosphatase) and overall (ATPase, reductase) activities of BCR. Addition of the substrate BCoA to reduced and phosphorylated BCR resulted in a six- to sevenfold stimulation of the phosphatase activity, which again was in good accordance with the BCoA-dependent increase of the overall ATPase activity. The chemical properties of the formed enzyme-phosphate were indicative for a high-energy phosphoamidate (e.g., histidine-phosphate or lysine-phosphate) [50].

The results obtained concerning the electron activating machinery of BCR are summarised in a proposal for the catalytic cycle (Fig. 6). Depending on the presence or absence of the substrate BCoA, two catalytic cycles (referred to as cycle I and cycle II) can be distinguished. Both start with the reduced and nucleotide-bound enzyme
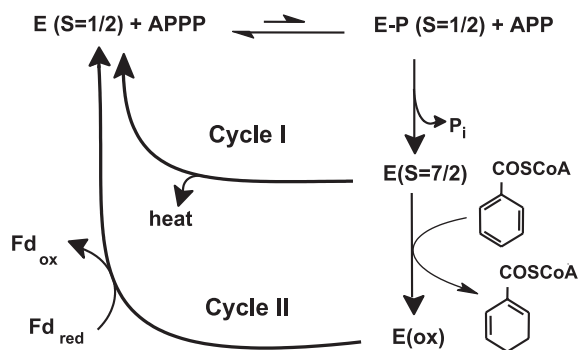

Fig. 6. Proposed catalytic cycle of ATP-driven electron transfer in BCR. Cycle I operates in reduced BCR in the absence of a reducible substrate, and cycle II operates in reduced BCR in the presence of BCoA. APPP = adenosine triphosphate, APP = adenosine diphosphate. Note that for full reduction of BCoA, the cycle has to run twice.

(S = 1/2 state of a [4Fe-4S]$^{+1}$ cluster, 2 ATP/enzyme); in both cases, an enzyme-phosphate is transiently formed. The equilibrium of this reaction is far on the side of ATP formation as evidenced by the steady state concentration of the formed enzyme-phosphate during the kinase reaction. Note that, e.g., the free energy of histidine-phosphate formation from ATP is clearly positive ($\Delta G > 10$ kJ mol^{-1}). As the switch from the S = 1/2 to the S = 7/2 state requires the coupling to an exergonic process, hydrolysis of the formed enzyme-phosphate should induce the necessary conformational change. In the absence of BCoA, no internal electron transfer takes place and the S = 7/2 high-spin [4Fe-4S]$^{+1}$ cluster switches back to the S = 1/2 state. This futile ATPase cycle is thought to continuously operate albeit at a reduced rate compared to the one coupled to electron transfer. BCoA stimulates the rate of ATP hydrolysis by a factor of 6 to 7, suggesting substrate-dependent conformational changes [9,24]. These changes should enable the coordinated sequence of low-potential electron generation and unidirectional transfer of these to the aromatic ring.

3.5. Mechanism of benzene ring reduction

If enzymatic BCoA reduction proceeds in a Birch-like mechanism, the first electron transfer to the substrate yielding a cyclohexadienoyl-CoA radical anion should be rate-limiting. For this reason, a transition state with an electron distribution similar to that of the cyclohexadienoyl-CoA radical anion was proposed [21]. The electron distribution was calculated ab initio and compared with that of the neutral substrate. The difference in the electron distribution between the radical anion and the neutral compound showed that—next to the oxygen and sulfur heteroatoms—excess of electron density is also located in the *ortho-* and *para*-position of the benzene ring (Fig. 7A). In a kinetic study, various BCoA analogues with altered electronic properties were used to probe the postulated Birch reduction mechanism in BCR catalysis [21]. Depending on the presence of electron donating or withdrawing functionalities, the radical anion transition state should be stabilised or destabilised, which should affect the rate of reduction. The relative differences in reduction rate and binding to the enzyme between various substrate analogues indicate that, indeed, the first electron transfer represents a rate-limiting step. The following examples are representative for the main tendencies found (see Fig. 7B–D): (i) for *ortho*-substituted BCoA derivatives, k_{cat} and K_m increased with the electron acceptor strength of the substituents (F>Cl=H>OH>NH$_2$). As the K_m increased in parallel, steric effects could not account for the differences in the reduction rates. E.g., 2-fluorobenzoyl-CoA was 13 times faster reduced than 2-aminobenzoyl-CoA although the affinity of BCR was approximately eightfold lower for the fluorinated than for the aminated compound. (ii) Among the isomers of mono-substituted analogues, the
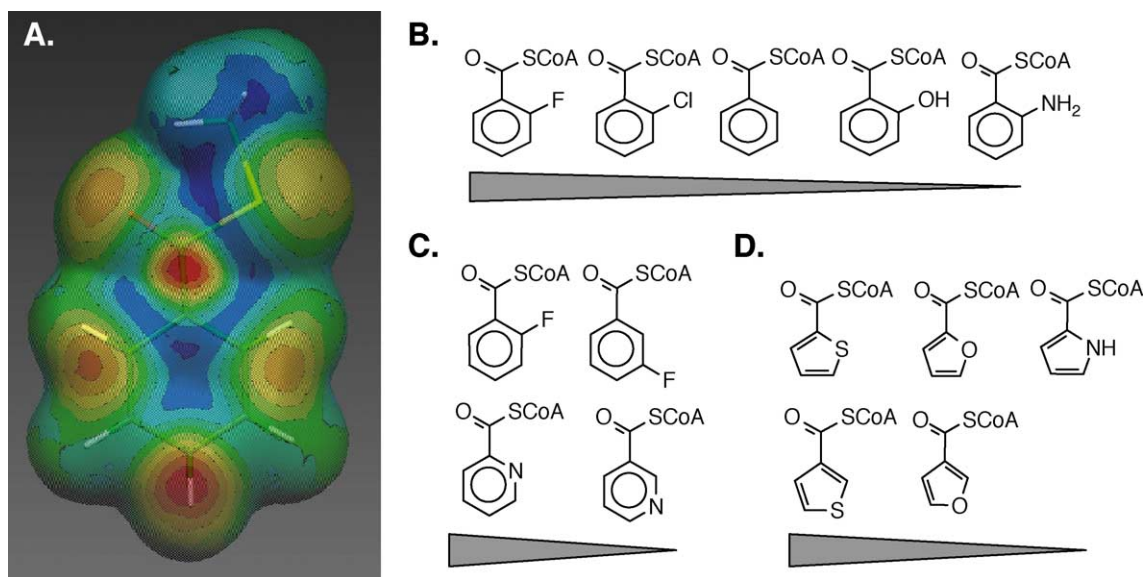
Fig. 7. Kinetic data supporting a 'Birch-like' mechanism in BCR catalysis. (A) Map of the B3LYP/6-31+G(d,p) difference electron density between the benzoic acid methylthiol ester radical anion and BCoA. The electron density is illustrated by the electrostatic potential (red pole of the spectrum = high electron density, blue pole of the spectrum = low electron density). (B) Order of k_{cat} values of *ortho*-substituted BCoA analogues; the bar represents the decrease in reduction rate with decreasing electron withdrawing character of the functionality. (C) As B using position isomers of fluorinated BCoA derivatives and of pyridine-1-carbonyl-CoA. (D) As B using five-ringed heteroaromatic coenzyme A thiol esters.

reduction rate was much higher in *ortho*- than in *meta*-position (e.g., 2-fluorobenzoyl-CoA was converted at a higher rate than 3-fluorobenzoyl-CoA). (iii) The order of reduction for heteroaromatic thiol esters was thiophene>furan>pyrrole, the 2-isomers again being reduced much more readily than the 3-isomers. The results were in good accordance with a Birch reduction mechanism. In addition, they ruled out alternative chemistries of substrate reduction, such as hydride or hydrogen atom addition. Note that no *para*-substituted BCoA derivative was used by BCR. As *para*-substituted BCoA analogues were bound to the enzyme the inability of BCR to reduce them is explained by a disabled protonation at this site, which, in turn, should negatively affect the first electron transfer [21] (see below).

Further analysis of the kinetic data by a Hammet plot excludes a pure polar mechanism in which electron- and proton transfer to the benzene moiety represent time-resolved steps [21]. The results rather suggest that electron transfer to the aromatic substrate is assisted by the simultaneous protonation at the *para*-position thereby avoiding the formation of a true radical anion intermediate. The first electron transfer could be further facilitated by partial protonation of the carbonyl oxygen (Fig. 8; note that a full protonation would result in the futile reduction to benzaldehyde). Ab initio calculations of a ketyl radical transition state model for methylmalonyl-CoA mutase showed that such a partial protonation can account for an increase in redox potential of ∼ 250 mV [51]. According to the modifications of the classical Birch reduction, the mechanism of BCR should be rather termed 'Birch-like' [21] (Fig. 8). A scheme for the energetics of the

catalyzed and non-catalysed first electron transfer is depicted in Fig. 9. The lowering of the redox potential gap between the electron donor ferredoxin and the dienoyl-CoA radical anion could be accomplished by (i) a lowering of the redox potential of the electrons to be transferred to the aromatic ring (S = 7/2 state formation driven by ATP hydrolysis), and by (ii) a rise of the redox potential of the aromatic substrate (concerted protonation and electron transfer steps in addition to a partial protonation of the enzyme-bound substrate; Fig. 9).

The proposed Birch-like reduction mechanism is supported by spectroscopic evidence for transient radical intermediates during catalysis. Reduced BCR was mixed with its substrates MgATP and BCoA after which EPR spectra were recorded within the time-scale of a single BCoA turnover (3 s at 20 °C and pH 8.2; [52]). In an early phase (<0.2 s), the partially reduced $[4Fe-4S]^{+1}$ clusters were gradually oxidised indicating internal electron trans-
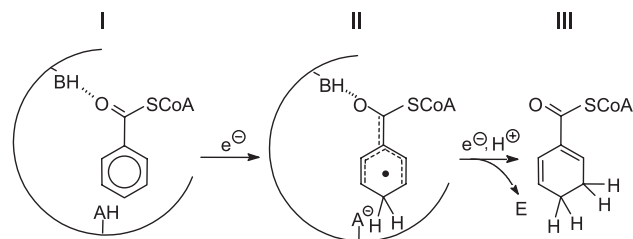

Fig. 8. Proposed modified 'Birch-like' mechanism of BCR. (I) Model of BCoA binding to BCR. Prior to reduction, the carbonyl oxygen is partially protonated by a weakly acidic proton. (II) Simultaneous with the electron transfer to BCoA, a bond to the *para*-attacking proton is formed. (III) Finally, the neutral cyclohexadienoyl intermediate is reduced by an additional electron and proton transfer. E = BCR.
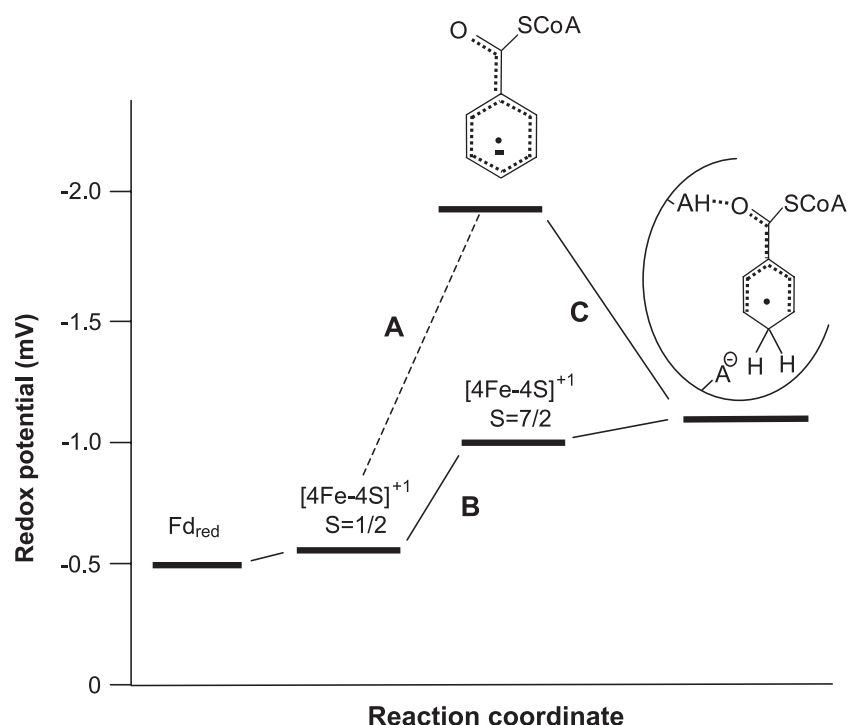
Fig. 9. Scheme for the energetics of the first electron transfer in BCR catalysis. Electrons are transferred from the donor reduced ferredoxin to the electron accepting [4Fe-4S] cluster of BCR (for ferredoxin the average E' ° of both [4Fe-4S] clusters was used [10]). (A) Redox gap between the BCR cluster and a free dienoyl-CoA radical anion. (B) ATP hydrolysis-dependent lowering of the redox potential of a [4Fe-4S]$^+$ cluster [48]. (C) Estimated rise of BCoA reduction potential by (i) simultaneous protonation and electron transfer avoiding the formation of a highly reactive radical anion species and by (ii) partial protonation of the carbonyl oxygen atom.

fer reactions (Fig. 10). In the late phase (2 s) novel EPR signals showed up. A difference EPR spectrum between the 2 s minus the 0.2 s sample revealed the rise of a novel EPR signal. The isotropic line shape of this signal was typical for a radical species (Fig. 10B). However, in comparison to a free organic radical the g_{av} of 2.017 was clearly shifted to the low-field region being rather typical for sulfur centred radical species. Together with other EPR parameters (e.g., temperature dependence and microwave power saturation), the signal fitted best with a protein-derived disulfide radical anion strongly interacting with a fast relaxing paramagnet (e.g., with one of the [4Fe-4S]$^{+1}$ clusters). A highly similar EPR signal was obtained in the presence of the competitive inhibitor 4-fluoroben-
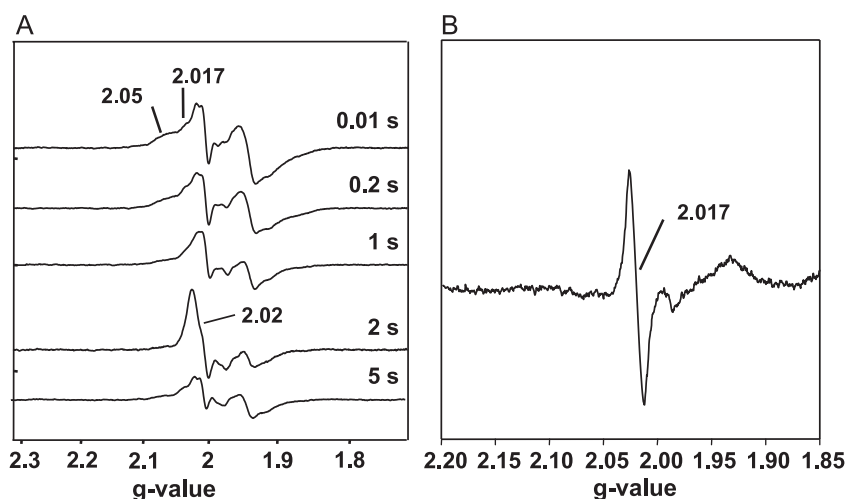

Fig. 10. Representative single turnover EPR spectra of dithionite-reduced BCR after addition of BCoA and MgATP recorded at 18 K, and 2 mW. BCR (340 μM) was anaerobically mixed with BCoA (340 μM) and MgATP (10 mM). Samples taken at different time points (as indicated) were frozen after which EPR spectra were recorded. (A) Representative spectra; the numbers refer to g-values. (B) Difference EPR spectrum of the sample taken at 2 s minus the one taken at 0.2 s.

zoyl-CoA (Möbitz and Boll, unpublished data). The *para*-fluoro atom largely decreases the electron density at C-4 of the putative radical intermediate, which negatively affects the necessary simultaneous protonation at this position. As a result, the endergonic first electron transfer to the aromatic ring might be no longer favourable; the activated electron could be trapped at the disulfide radical anion/[4Fe-4S] cluster site.

Midpoint potentials of disulfide radical anion model compounds are extremely low (e.g., $E'°$ is approximately -1.6 V for the dithioerythritol disulfide radical anion) [53]. Therefore, a protein-derived disulfide radical anion would be an attractive candidate for a low-potential electron donor for enzymatic benzene ring reduction. Interestingly, a disulfide radical anion has been identified by high-field pulsed EPR spectroscopy in the R1 mutant E441Q of *Escherichia coli* ribonucleotide reductase [54]. The role of such a low-potential species might be similar in ribonucleotide reductase and BCR catalysis: the disulfide radical anion is assumed to reduce the chemically closely related ketone (ribonucleotide reductase) or thiol ester (BCR) functionalities to a disulfide and a radical species.

The nature of the putative disulfide radical anion/[4Fe-4S] species in BCR is still speculative. In radical/*S*-adenosylmethionine (SAM) enzymes, a direct coordination of SAM to a [4Fe-4S] cluster by the sulfur atom has been demonstrated [55–57]. In these enzymes, SAM becomes transiently cleaved to a 5′ deoxyadenosyl radical and thereby functions as a radical initiator [58,59]. Notably, this cleavage requires the addition of a low-potential electron from a $[4Fe-4S]^{+1}$ cluster. The difficult reductive cleavage of SAM is facilitated by the direct coordination of the substrate enabling an inner sphere electron transfer from the $[4Fe-4S]^{+1}$ cluster to the sulfonium substrate. In BCR, a direct coordination of the thiol ester functionality of BCoA to a [4Fe-4S] cluster could have a similar function. However, experimental evidence for a direct coordination of BCoA to a [4Fe-4S] species is lacking.

A true organic substrate radical species in BCR has not been observed under any condition which might be due to its high reactivity. It is rather assumed that BCR—similar to nitrogenase—'stores' an activated low-potential electron at a more stabilised site before the second electron transfer to BCoA takes place. Such a site could consist of a disulfide radical anion interacting with a [4Fe-4S] cluster. The clear assignment of the $g = 2.017$ EPR signal by further spectroscopic techniques will be crucial for the elucidation of the electron transfer events at the active site of BCR.

4. 4-HBCR (dehydroxylating)

4.1. General properties

As *para*-substituted BCoA derivatives cannot be directly reduced by BCR (see above), an additional type of reductases should exist which reductively removes the substituents prior to ring reduction [21]. 4-HBCR from *T. aromatica* catalyzes the reductive dehydroxylation of 4-HBCoA to BCoA; two electrons are transferred from the reduced electron donor ferredoxin to the substrate (Fig. 11A) [11,12]. The same reduced ferredoxin serves as electron donor for 4-HBCR and BCR.

4-HBCR from *T. aromatica* has a molecular mass of 270 kDa and consists of three subunits of 82 (a), 35 (b) and 17 kDa (c), suggesting an (abc)$_2$ composition (Fig. 11B; Refs. [11,12]). The enzyme contains two $[2Fe-2S]^{+1/+2}$ clusters, one $[4Fe-4S]^{+1/+2}$ cluster, one FAD, and one molybdopterin cytosine dinucleotide cofactor per monomer [60]. The recent claim that 4-HBCR contains a molybdopterin-mononucleotide cofactor could not be confirmed in the crystal structure and might represent an artefact of sample preparation (unpublished results). 4-HBCR is inactivated by cyanide, which is typical for enzymes of the xanthine oxidase (XO) family containing a molybdenum cofactor. Cyanide reacts with a Mo-coordinated inorganic sulfur atom yielding thiocyanate and inactivated desulfo-enzyme (for recent reviews on XO enzyme family, see Refs. [61–63]).

4.2. Similarities to other enzymes

The genes coding for the three subunits of 4-HBCR were cloned and sequenced in *T. aromatica* and in the phototrophic bacterium *R. palustris* [12,64]; the amino acid sequences of the subunits of the individual enzymes showed 47–62% identity. The three structural genes are flanked in both organisms by genes coding for transcriptional regulators and a permease (*T. aromatica*) [12] or a 4-HBCoA synthetase
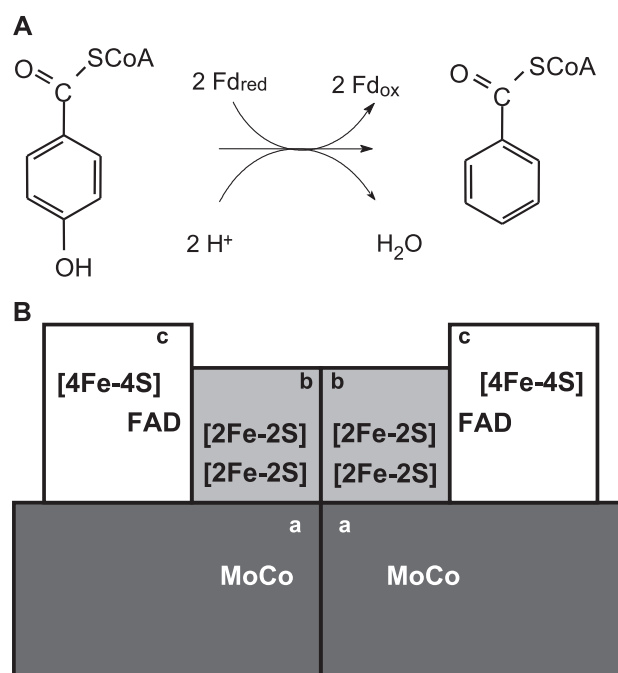

Fig. 11. Properties of 4-HBCR from *T. aromatica*. (A) Reaction catalyzed. (B) Subunit/cofactor architecture.

and an ABC-transporter (*R. palustris*) [64]. The whole genome of *M. magnetotacticum* also contains three open reading frames coding for proteins with very high similarities to 4-HBCR from *T. aromatica* with 85% (a), 70% (b) and 91% (c) identities. In addition, 4-HBCR has amino acid sequence similarities (25–35% identity) to all members of the XO family of molybdenum cofactor-containing enzymes (e.g., xanthine dehydrogenases, aldehyde oxidases, CO dehydrogenases from many different organisms).

4.3. General architecture

Based on the similarities to XO members with known structures (CO dehydrogenase [65], xanthine dehydrogenase [66] and aldehyde oxidase [67]), the following common subunit/cofactor architecture is suggested for 4-HBCR from *T. aromatica* (Fig. 11B): (i) as in all other XO family enzymes, the large a-subunit of 4-HBCR harbours the molybdenum cofactor; this is the site where catalysis takes place. (ii) The b-subunit contains a flavin binding domain of the vanillyl alcohol oxidase family; it is supposed to bind one FAD. Note that this subunit is not present in all XO members (e.g., aldehyde oxidase). (iii) The small subunit harbours eight conserved cysteines coordinating two $[2Fe\text{-}2S]^{+1/+2}$ clusters which mediate electron transfer between the flavin and the molybdenum cofactor.

In spite of the high similarities, some properties of 4-HBCR are unique among the XO family: (i) the β-subunit contains an additional loop consisting of approximately 40 amino acids in which a $[4Fe\text{-}4S]^{+1/+2}$ cluster is coordinated. This cluster is considered to play a crucial role in the reversed electron transfer by mediating electrons from the low-potential donor, reduced ferredoxin, to the other redox centres. None of the so far characterised XO members contains this cluster-loop. (ii) 4-HBCR is the only member of the XO family whose function is to catalyse the reduction of the substrate. All other XO family enzymes catalyse the two electron oxidation of their substrates by water using usually NAD^+ or oxygen as electron acceptors. The most conceivable mechanism of 4-HBCR is a Birch-like reduction by means of radical intermediates (see Fig. 2). Next to the pyrogallol-phloroglucinol transhydroxylase [68], it is the only Mo-enzyme for which a radical mechanism has been proposed. (iii) The substrate of 4-HBCR is exceptionally large; the coenzyme A thiol ester is expected to have a specific binding site which should be missing in other XO family enzymes.

The presence of the cluster-loop containing five cysteines was considered as a distinguishing feature of 4-HBCR. However, various sequenced microbial genomes contain genes coding for β-subunits of unknown XO-family enzymes, which, similar to 4-HBCR, contain such an extra cluster-loop (Table 2). These cluster loops comprise four to five cysteine residues, of which three can be aligned to cysteines of the cluster-loop in 4-HBCR. Notably, none of the organisms containing the genes for the XO-like enzymes

Table 2
Amino acid sequence alignment of the cluster-loop region in the b-subunit of 4-HBCRs with other enzymes containing the molybdenum cofactor

Organism	Amino acid sequence	Accession
Thauera aromatica 4-HBCR	^{113}ggnlcqdtrctfynqseww----rsgngyclkykg-dkch-vivksdrcyatyhgdvapalmv^{169}	AA05039
Magnetospirillum magnetotacticum 4-HBCR	^{113}ggnlcqdtrcvfynqseww----rsgngfclkyeg-dkch-vvvksdrcyatyhgdvapalmv^{169}	ZP_00054039
Rhodopseudomonas palustris 4-HBCR	^{113}ggnlcldtrciyynqseww----rransyclknrg-eich-vapkgnrchaafsgdlapallv^{169}	AAB42209
Burkholderia fungorum unknown protein	^{110}ggnllqrtrcgyfydtaftqnkrtpgsgcaaldghnrthailgaspqciavmpsdmsvalaa^{172}	ZP_00033754
Sinorhizobium meliloti unknown protein	^{110}agnlmqrtrclyfydha-archkrapgagcdaiggfnrmhailgasdsciathpsdmcvalaa^{172}	NP_436922
Agrobacterium tumefaciens unknown protein	^{109}ggnilqrtrcryfydna-archkrqpnsgcdalegfnryhailgasescvathpsdmcvalva^{170}	NP_396433
Oligotropha carboxydovorans CODH	^{113}ggnlaangd------------------------pgndm-palmq^{131}	P19920
Milk XO	^{130}ggniitas--------------------------pisdlnpvfma^{148}	10835430

CODH, carbon monoxide dehydrogenase. The cysteines putatively involved in Fe/S-cluster coordination are depicted with a black/grey background. The amino acid sequences of enzymes 2–6 are deduced from the gene sequences.

are known to use aromatic compounds as growth substrates anaerobically (e.g., *Sinorhizobium meliloti*, *Agrobacterium tumefaciens*, *Burkholderia fungorum*). This finding implies that further types of XO-type enzymes exist, which may catalyze the reductive dehydroxylation of their substrates by means of an additional Fe/S-cluster.

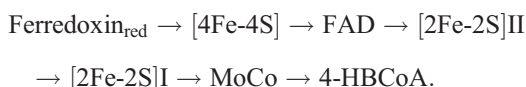### 4.4. Spectroscopic and electrochemical properties—evidence for a reversed electron flow

The redox centres of 4-HBCR were studied in detail by Mössbauer and EPR spectroscopy [60]. The EPR properties of the $[2Fe-2S]^{+1}$, FAD semiquinone and the Mo(V) species were similar to those of the other XO family members. The Mo(V) species showed a strong hyperfine coupling with one or more proton(s). This coupling was not observed in the Mo(V) signal from the cyanide treated desulfo-enzyme, which is typical for the loss of the cyanolysable -SH ligand of molybdenum. At potentials below -420 mV, the $[4Fe-4S]^{+1/+2}$ cluster became reduced (paramagnetic), which strongly affected the EPR properties of all other redox centres. For instance, the usual $S = 1/2$ EPR signals of the $[2Fe-2S]^{+}$ cluster totally disappeared and the $S = 1/2$ Mo(V) species showed an increased relaxation behaviour which indicated a strong magnetic interaction with the fast relaxing $[4Fe-4S]^{+1}$ cluster [60]. Especially the latter effect was surprising as the distance between the [4Fe-4S] cluster and the Mo(V) species is >40 Å (as deduced from the crystal structure; Unciuleac and Boll, unpublished results). This phenomenon cannot be sufficiently explained so far and might be due to a kind of super exchange of electrons by means of all redox centres.

EPR redox titrations studies revealed that the redox potentials of the $[2Fe-2S]^{+1/+2}$ clusters of 4-HBCR are in the range of other XO family members ($E'° \sim -200$ mV– -300 mV, Table 3). In contrast, the redox transition of the FADH/FADH· (-470 mV) and Mo(IV)/(V) (-500 mV) couples are exceptionally low compared to other XO family members and are in the range of the additional $[4Fe-4S]^{+1/+2}$ cluster (-465 mV; Table 3) [60]. Note that the low potentials of the Mo(IV/V) and Mo(V/VI) transitions of aldehyde oxidase were determined for the catalytically nonrelevant "slow" Mo(V) EPR signal [69,70], whereas in 4-HBCR they were determined for the catalytically relevant "rapid signal".

The following electron transfer chain is most plausible for all XO family members investigated so far [63]:

$$\text{Substrate} \rightarrow \text{MoCo} \rightarrow [2Fe-2S]I \rightarrow [2Fe-2S]II$$

$$\rightarrow \text{FAD} \rightarrow \text{NAD}/O_2$$
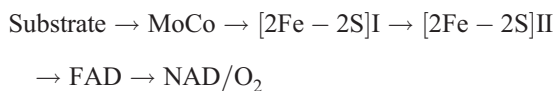
The existence of this electron transfer chain is also indicated by the redox potentials of the individual redox centres. Although there are variations in the individual enzymes, in all cases the redox potential of the donor couple (CO_2/CO, carboxylic acid/aldehyde, uric acid/xanthine) is clearly more negative than that of the acceptor couple (e.g., NAD/NADH; O_2/H_2O_2). Thus, the overall reaction is mostly irreversible in members of the XO family. In contrast, the redox properties and proposed molecular architecture of the cofactors in 4-HBCR suggest the following inverted electron transfer chain:

$$\text{Ferredoxin}_{red} \rightarrow [4Fe-4S] \rightarrow \text{FAD} \rightarrow [2Fe-2S]II$$

$$\rightarrow [2Fe-2S]I \rightarrow \text{MoCo} \rightarrow \text{4-HBCoA}.$$

The electron transfer chain starts with the reduced electron donor ferredoxin harbouring two $[4Fe-4S]^{+1/+2}$ clusters with an average midpoint potential of ~ -500 mV [49]. This potential is sufficient low for transferring electrons to the primary acceptor, the oxidised $[4Fe-4S]^{+2}$ cluster. From the $[4Fe-4S]^{+1}$ cluster so formed, the electrons are transferred to the oxidised Mo-cofactor by means of the [2Fe-2S] I and II clusters. Compared to the other redox cofactors, the $[2Fe-2S]^{+1/+2}$ clusters have much more positive redox potentials resulting in a U-shaped energy-dependence of the electron transfer coordinate (Fig. 12). It is not clear whether the 'low-potential' FADH/semiquinone or the 'high-potential' semiquinone/FAD transitions is involved in this transfer. In both cases, the role of FAD is unusual as it mediates an electron transfer between two one-electron carriers and not between one- and two-electron redox centres.

Unfortunately, exact values for redox potentials of the 4-HBCoA/BCoA couple do not exist. The formation of benzoate and water from 4-hydroxybenzoate using molecular hydrogen as electron donor is highly exergonic ($\Delta G = -59$ kJ mol^{-1} corresponding to $E'° \sim +150$ mV for the 4-hydroxybenzoate/benzoate redox couple) as

Table 3
Redox potentials (mV) of cofactors from some enzymes of the XO family

Enzyme	[2Fe-2S] I	[2Fe-2S] II	[4Fe-4S]	FAD/FADH·	FADH·/FADH	Mo(VI)/Mo(V)	Mo(V)/Mo(IV)	Reference
4-HBCR	-205	-255	-465	-250	-470	-380	-500	[60]
XO (milk)	-280	-245	N.P.	-310	-220	-355	-335	[70]
XDH (cl)	-280	-275	N.P.	-345	-377	-357	-337	[70]
AOR (Ds)	-280	-285	N.P.	N.P.	N.P.	-415^a	-530^a	[71]

XDH (cl), xanthine dehydrogenase from chicken liver; AOR (Ds), aldehyde oxidase from *D. gigas*. N.P.—not present.
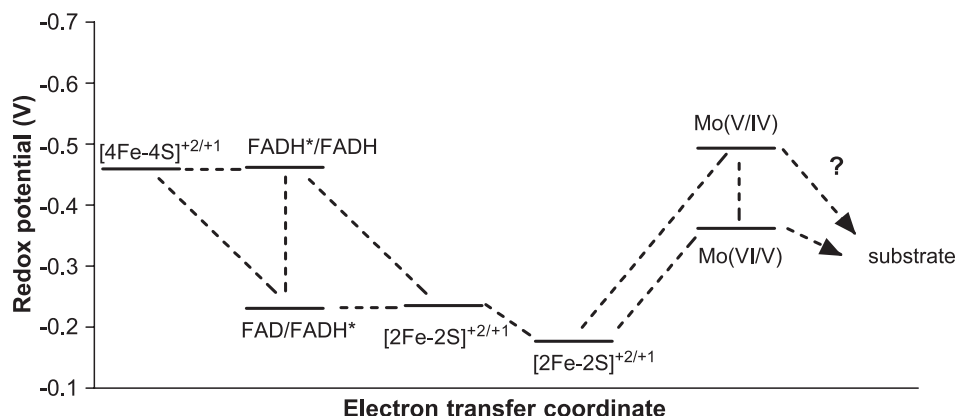 ^{a} Redox titration of the slow type EPR signal.

Fig. 12. Schematic presentation of the electron transfer steps between the individual cofactors of 4-HBCR including their redox potentials. Note that the electron transfer coordinate does not represent real distances between the redox centres. It is not clear which of the two possible redox transitions of FADH depicted in the scheme is involved in the electron transfer from $[4Fe-4S]^{+1}$ to the $[2Fe-2S]^{+2}$ centres. The exact redox potential of the substrate/product couple is unknown. Note that the redox potential for the overall reaction will be more positive than the Mo(IV/V) couple with the first electron transfer to the substrate requiring a more negative potential than the second one.

calculated from the free energy of formation from the elements [72]. However, from mechanistic reasons the first electron transfer to the aromatic moiety of 4-HBCoA will be extremely difficult (Fig. 2). Thus, very low potentials are required to make the dehydroxylation process possible at physiological rates.

4.5. Mechanism of reductive dehydroxylation

A mechanism involving radical intermediates is untypical for molybdopterin containing enzymes. In the following, a catalytic cycle is presented which combines the postulated special one-electron chemistry involved in the dehydroxylation of a phenolic compound with the typical XO-family type of molybdenum cofactor coordination of 4-HBCR. In addition to the two sulfur ligands of the dithiolene group of the molybdopterin cofactor, the Mo(VI) atom is coordinated by one oxo-, one sulfur- and one hydroxy- (or water) ligand. The catalytic cycle presented runs counterclockwise to the catalytic cycle of all other xanthine-oxidase-type enzymes; it consists of five distinguishable steps I–V (Fig. 13) [60].
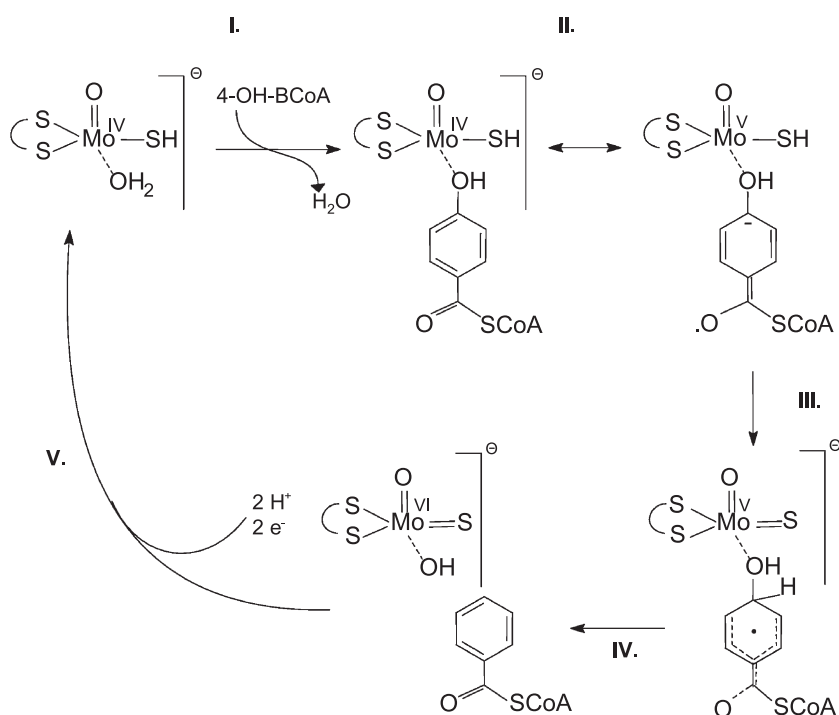

Fig. 13. Hypothetical catalytic cycle of 4-HBCR. The cycle runs counterclockwise to that of usual XO family members.

4.5.1. Step I: Binding of the substrate

In the absence of the substrate, a water molecule is coordinated to the Mo atom (as deduced from the crystal structure; Unciuleac and Boll, unpublished results). 4-HBCoA will most probably bind via the *para*-hydroxy group not to the oxidised Mo(VI) but to the fully reduced Mo(IV) species with a concomitant displacement of the water ligand at the Mo atom.

4.5.2. Step II: Charge transfer from Mo-cofactor to the substrate generating a radical anion and a Mo (V) species

Such charge transfer seems plausible because of the unusual low reduction potential of the Mo(V)/Mo(IV) redox couple. Note that the radical anion can be stabilised not only by the aromatic ring including the carbonyl functionality of the thiol ester, but also by the dithiolene group. The radical anion could be further stabilised by a partial protonation at the carbonyl oxygen as it has been proposed for the analogous radical intermediate in BCR [21].

4.5.3. Step III: Protonation of the radical anion

The highly favourable protonation of the radical anion at the *para*-position will yield a free radical. This protonation is facilitated by the high electron density of the radical anion at the *para*-position of the aromatic ring. It is most likely that a Mo-coordinated -SH group is the ultimate proton donor for this reaction as the deprotonated sulfur atom is considered as proton acceptor in the reverse reaction of all other XO family members. In 4-HBCR the deprotonated sulfur atom is likely to be regenerated by a carboxyl proton from Glu^{726} which represents a conserved residue in close proximity to the Mo-coordinated sulfur atom in XO-family enzymes [66,67].

4.5.4. Step IV: Homolytic cleavage of the carbon-oxygen bond

Although this step yielding BCoA and a Mo(VI)-OH is considered to be mechanistically difficult, it will be largely driven by the rearomatization of the free radical species yielding BCoA and Mo-coordinated water. Alternatives to this homolytic cleavage, such as formation of a phenyl cation or a H_2O^+ species, are thermodynamically extremely unfavourable.

4.5.5. Step V: Reductive two-electron regeneration of the Mo(IV)

For the regeneration of Mo(IV), two electrons are transferred to the molybdenum centre.

5. Birch-like reductions in BCR and 4-HBCR catalysis—why so different ?

BCR and 4-HBCR appear to solve the problem of the difficult first electron transfer to their aromatic substrates in a different manner, which is reflected by their totally different architecture and cofactor content. It is proposed that in both cases, catalysis involves the stabilisation of a highly reactive radical species. The electron donating *para*-hydroxyl group of 4-HBCoA rather destabilises a putative benzene ring radical anion. For this reason, the redox potential for the first electron transfer should be rather lower for 4-HBCoA than for BCoA. In 4-HBCR the direct coordination of the substrate to the Mo atom via the hydroxyl group enables the delocalization of the radical anion/free radical, probably including the dithiolene group of the pterin cofactor. In contrast, there is no evidence for a direct binding of BCoA to BCR. In BCR the non-covalent stabilisation/delocalization of a reactive radical intermediate by interaction with the putative disulfide radical/[4Fe-4S]$^{+1}$ complex will be much weaker than in case of 4-HBCR. As a result, the redox potential required for the first electron transfer will be much lower in case of BCoA than for 4-HBCoA. Consequently, BCR catalysis requires the input of external energy to promote electron transfer at a physiological rate, whereas 4-HBCR does not.

References

[1] S. Harayama, M. Kok, E.L. Neidle, Functional and evolutionary relationships among diverse oxygenases, Annu. Rev. Microbiol. 46 (1992) 601–656.

[2] M. Boll, G. Fuchs, H. Heider, Anaerobic metabolism of aromatic compounds, Curr. Opin. Chem. Biol. 6 (2002) 604–611.

[3] J. Gibson, C.S. Harwood, Metabolic diversity in aromatic compound utilization by anaerobic microbes, Annu. Rev. Microbiol. 56 (2002) 345–369.

[4] B. Schink, B. Philipp, J. Müller, Anaerobic degradation of phenolic compounds, Naturwissenschaften 87 (2000) 12–23.

[5] C.S. Harwood, G. Burchhardt, H. Herrmann, G. Fuchs, Anaerobic metabolism of aromatic compounds via the benzoyl-CoA pathway, FEMS Microbiol. Rev. 22 (1999) 439–458.

[6] J.D. Haddock, J.G. Ferry, Purification and properties of phloroglucinol reductase from *Eubacterium oxidoreducens* G-41, J. Biol. Chem. 264 (1989) 4423–4427.

[7] W. Reichenbecher, B. Schink, *Desulfovibrio inopinatus*, sp. nov., a new sulfate-reducing bacterium that degrades hydroxyhydroquinone, Arch. Microbiol. 168 (1997) 338–344.

[8] C. Kluge, A. Tschech, G. Fuchs, Anaerobic metabolism of resorcyclic acids (*m*-dihydroxybenzoic acids) and resorcinol (1,3-benzenediol) in a fermenting and in a denitrifying bacterium, Arch. Microbiol. 155 (1990) 68–74.

[9] M. Boll, G. Fuchs, Benzoyl-coenzyme A reductase (dearomatizing), a key enzyme of anaerobic aromatic metabolism. ATP dependence of the reaction, purification and some properties of the enzyme from *Thauera aromatica* strain K172, Eur. J. Biochem. 234 (1995) 921–933.

[10] M. Boll, G. Fuchs, Identification and characterization of the natural electron donor ferredoxin and of FAD as a possible prosthetic group of

benzoyl-CoA reductase (dearomatizing), a key enzyme of anaerobic aromatic metabolism, Eur. J. Biochem. 251 (1998) 946–954.

[11] R. Brackmann, G. Fuchs, Enzymes of anaerobic metabolism of phenolic compounds—4-Hydroxybenzoyl-CoA reductase (dehydroxylating) from a denitrifying *Pseudomonas species*, Eur. J. Biochem. 213 (1993) 563–571.

[12] K. Breese, G. Fuchs, 4-Hydroxybenzoyl-CoA reductase (dehydroxylating) from the denitrifying bacterium *Thauera aromatica*. Prosthetic groups, electron donor, and genes of a member of the molybdenum-flavin-iron-sulfur proteins, Eur. J. Biochem. 251 (1998) 916–923.

[13] A.J. Birch, H. Smith, Reduction by metal-amine solutions: application in the synthesis and determination of structure, Q. Rev. Chem. Soc. Lond. 12 (1958) 17–33.

[14] A.J. Birch, A.K. Hinde, L. Radom, A theoretical approach to the Birch reduction. Structures and stabilities of the radical anions of substituted benzenes, J. Am. Chem. Soc. 102 (1980) 3370–3376.

[15] J. Mortensen, J. Heinze, Die elektrochemische Reduktion von Benzol—erste direkte Bestimmung des Redoxpotentials, Angew. Chem. 96 (1984) 64–65.

[16] U. Altenschmid, B. Oswald, G. Fuchs, Purification and characterization of benzoate-coenzyme A ligase and 2-aminobenzoate-coenzyme A ligases from a denitrifying Pseudomonas sp., J. Bacteriol. 137 (1991) 5494–5501.

[17] T. Biegert, U. Altenschmidt, C. Eckerskorn, G. Fuchs, Enzymes of anaerobic metabolism of phenolic compounds. 4-Hydroxybenzoate-CoA ligase from a denitrifying Pseudomonas species, Eur. J. Biochem. 213 (1993) 555–561.

[18] W. Buckel, R. Keese, One electron reactions of CoASH esters in anaerobic bacteria, Angew. Chem., Int. Ed. Engl. 34 (1995) 1502–1506.

[19] M. Boll, D. Laempe, W. Eisenreich, A. Bacher, T. Mittelberger, J. Heinze, G. Fuchs, Non-aromatic products from anoxic conversion of benzoyl-CoA with benzoyl-CoA reductase and cyclohexa-1,5-diene-1-carbonyl-CoA hydratase, J. Biol. Chem. 275 (2000) 21889–21895.

[20] J. Koch, W. Eisenreich, A. Bacher, G. Fuchs, Products of enzymatic reduction of benzoyl-CoA, a key reaction in anaerobic aromatic metabolism, Eur. J. Biochem. 205 (1993) 195–202.

[21] H. Möbitz, M. Boll, A Birch-like mechanism in enzymatic benzoyl-CoA reduction—a kinetic study of substrate analogues combined with an ab initio model, Biochemistry 41 (2002) 1752–1758.

[22] U. Feil, Anaerober Stoffwechsel von 2-Aminobenzoat in denitrifizierenden Bakterien, PhD thesis, University of Freiburg, Institut for Biology II, 1998.

[23] D. Laempe, M. Jahn, K. Breese, H. Schägger, G. Fuchs, Anaerobic metabolism of 3-hydroxybenzoate by the denitrifying bacterium *Thauera aromatica*, J. Bacteriol. 183 (2001) 968–979.

[24] M. Boll, S.J.P. Albracht, G. Fuchs, Benzoyl-CoA reductase (dearomatizing), a key enzyme of anaerobic aromatic metabolism. A study of adenosinephosphate activity, ATP stoichiometry of the reaction and EPR properties of the enzyme, Eur. J. Biochem. 244 (1997) 840–851.

[25] M. Boll, G. Fuchs, C. Meier, A.X. Trautwein, D.J. Lowe, EPR and Mössbauer studies of benzoyl-CoA reductase, J. Biol. Chem. 275 (2000) 31857–31868.

[26] K. Breese, M. Boll, J. Alt-Mörbe, H. Schägger, G. Fuchs, Genes coding for the benzoyl-CoA pathway of anaerobic aromatic metabolism in the bacterium *T. aromatica*, Eur. J. Biochem. 256 (1998) 148–154.

[27] E. Dörner, M. Boll, Properties of 2-oxoglutarate:ferredoxin oxidoreductase from *Thauera aromatica* and its role in enzymatic reduction of the aromatic ring, J. Bacteriol. 184 (2002) 3975–3983.

[28] D. Laempe, W. Eisenreich, A. Bacher, G. Fuchs, Cyclohexa-1,5-diene-1-carboxyl-CoA hydratase, an enzyme involved in anaerobic metabolism of benzoyl-CoA in the denitrifying bacterium *Thauera aromatica*, Eur. J. Biochem. 255 (1998) 618–627.

[29] D. Laempe, M. Jahn, G. Fuchs, 6-Hydroxycyclohexa-1-ene-1-carbonyl-CoA dehydrogenase and 6-oxocyclohex-1-ene-1-carbonyl-CoA hydrolase, enzymes of the benzoyl-CoA pathway of anaerobic aro-matic metabolism in the denitrifying bacterium *Thauera aromatica*, Eur. J. Biochem. 263 (1999) 420–429.

[30] U. Härtel, E. Eckel, J. Koch, G. Fuchs, D. Linder, W. Buckel, Purification of glutaryl-CoA dehydrogenase from Pseudomonas sp., an enzyme involved in the anaerobic degradation of benzoate, Arch. Microbiol. 159 (1993) 174–181.

[31] J.H. Hurley, The sugar kinase/heat shock protein 70/actin superfamily: Implications of conserved structure for mechanism, Annu. Rev. Biophys. Biomol. Struct. 25 (1996) 137–162.

[32] K.A. Buss, D.R. Cooper, C. Ingram-Smith, J.G. Ferry, D.A. Sanders, M.S. Hasson, Urkinase: structure of acetate kinase, a member of the ASKHA superfamily of phosphotransferases, J. Bacteriol. 183 (2001) 680–686.

[33] G.E. Schulz, Induced-fit movements in adenylate kinases, Curr. Opin. Struck. Biol. 2 (1992) 61–67.

[34] P.L. Dutton, W.C. Evans, The metabolism of aromatic compounds by *Rhodopseudomonas palustris*: a new reductive method of aromatic ring metabolism, Biochem. J. 123 (1969) 525–536.

[35] P.G. Egland, D.A. Pelletier, M. Dispensa, J. Gibson, C.S. Harwood, A cluster of bacterial genes for anaerobic benzene ring biodegradation, Proc. Natl. Acad. Sci. 94 (1997) 6484–6489.

[36] D.C. Rees, J.B. Howard, Nitrogenase: standing at the crossroads, Curr. Opin. Chem. Biol. 4 (2000) 559–566.

[37] W. Buckel, Unusual dehydrations in anaerobic bacteria: considering ketyls (radical anions) as reactive intermediates in enzymatic reactions, FEBS Lett. 389 (1996) 20–24.

[38] W. Buckel, Unusual enzymes involved in five pathways of glutamate fermentation, Appl. Microbiol. Biotechnol. 57 (2001) 263–273.

[39] M. Hans, J. Sievers, U. Müller, E. Bill, J.A. Vorholt, D.W. Linder, Buckel, 2-Hydroxyglutaryl-CoA dehydratase from *Clostridium symbiosum*, Eur. J. Biochem. 265 (1999) 404–414.

[40] R. Dutscho, G. Wohlfahrth, P. Buckel, W. Buckel, Cloning and sequencing of the genes of 2-hydoxyglutaryl-CoA dehydratase from *Acidaminococcus fermentans*, Eur. J. Biochem. 181 (1989) 741–746.

[41] K.P. Locher, M. Hans, A.P. Yeh, B. Schmid, W. Buckel, D.C. Rees, Crystal structure of the *Acidaminococcus fermentans* 2-hydroxyglutaryl-CoA dehydratase component A, J. Mol. Biol. 307 (2001) 297–308.

[42] M. Hans, E. Bill, I. Cirpus, A.J. Pierik, M. Hetzel, D. Alber, W. Buckel, Adenosine triphosphate-induced electron transfer in 2-hydroxyglutaryl-CoA dehydratase from *Acidaminococcus fermentans*, Biochemistry 41 (2002) 5873–5882.

[43] S. Dickert, A.J. Pierik, W. Buckel, Molecular characterization of phenyllactate dehydratase and its initiator from *Clostridium sporogenes*, Mol. Microbiol. 44 (2002) 49–60.

[44] H. Möbitz, T. Friedrich, M. Boll, Substrate binding and reduction of benzoyl-CoA reductase: evidence for nucleotide-dependent conformational changes, Biochemistry (in press).

[45] J. Gaillard, J.-M. Moulis, P. Auric, J. Meyer, High-multiplicity spin states of 2[4Fe-4Se]$^+$ clostridial ferredoxins, Biochemistry 25 (1985) 464–468.

[46] W.R. Hagen, M. Wassink, R.R. Eady, B.E. Smith, M. Haaker, Quantitative EPR of an $S = 7/2$ system in thionine-oxidized MoFe proteins of nitrogenase. A redefinition of the P-cluster concept, Eur. J. Biochem. 169 (1987) 457–465.

[47] W.R. Hagen, EPR spectroscopy of iron-sulfur proteins, Adv. Inorg. Chem. 38 (1992) 165–222.

[48] C. Meier, Mössbauerspektroskopie an biomimetischen Modellkomplexen und nicht-Häm-Eisenproteinen, PhD thesis, University of Lübeck, Institut für Physik, 2001.

[49] M. Boll, G. Fuchs, G. Tilley, F.A. Armstrong, D.J. Lowe, Unusual spectroscopic and electrochemical properties of the 2[4Fe-4S] ferredoxin of *Thauera aromatica*, Biochemistry 39 (2000) 4929–4938.

[50] M. Unciuleac, M. Boll, Mechanism of ATP-driven electron transfer catalyzed by the benzene ring-reducing enzyme benzoyl-CoA reductase, Proc. Natl. Acad. Sci. 98 (2001) 13619–13624.

[51] D.M. Smith, B.T. Golding, L. Radom, Facilitation of enzyme-cata-

lyzed reactions by partial proton transfer: application to coenzyme-B_{12}-dependent methylmalonyl-CoA mutase, J. Am. Chem. Soc. 121 (1999) 1383–1384.

[52] M. Boll, G. Fuchs, D.J. Lowe, Single turnover EPR studies of benzoyl-CoA reductase, Biochemistry 40 (2001) 7612–7620.

[53] P.S. Surdhar, D.A. Armstrong, Reduction potentials and exchange reactions of thiyl radicals and disulfide anion radicals, J. Phys. Chem. 91 (1987) 6532–6537.

[54] C.C. Lawrence, M. Bennati, H.V. Obias, G. Bar, R.G. Griffin, J. Stubbe, High-field EPR detection of a disulfide radical anion in the reduction of cytidine 5′-diphosphate by the E441Q R1 mutant of *Escherichia coli* ribonucleotide reductase, Proc. Natl. Acad. Sci. 96 (1999) 8979–8984.

[55] C. Krebs, W.E. Broderick, T.F. Henshaw, J.B. Broderick, B.H. Huynh, Coordination of adenosylmethionine to a unique iron site of the [4Fe-4S] of pyruvate formate-lyase activating enzyme: a Mössbauer spectroscopic study. J. Am. Chem. Soc. 124 (2000) 912–913.

[56] M.M. Cosper, G.N.L. Jameson, R. Davydov, M.K. Eidsness, B.M. Hoffman, B.H. Huynh, M.K. Johnson, The [4Fe-4S]+2 cluster in reconstituted biotin synthase binds *S*-adenosyl-L-methionine, J. Am. Chem. Soc. 124 (2002) 14006–14007.

[57] M.M. Cosper, N.J. Cosper, W. Hong, J.E. Shokes, W.E. Broderick, J.B. Broderick, M.K. Johnson, R.A. Scott, Structural studies of the interaction of *S*-adenosylmethionine with the [4Fe-4S] clusters in biotin synthase and pyruvate formate-lyase activating enzyme, Prot. Sci. 12 (2003) 1573–1577.

[58] P.A. Frey, Radical mechanisms of enzymatic catalysis, Annu. Rev. Biochem. 70 (2001) 121–148.

[59] M. Fontecave, E. Mulliez, R. Ollagnier-de-Choudens, Adenosylmethionine as a source of 5′-deoxyadenosyl radicals, Curr. Opin. Chem. Biol. 5 (2001) 506–511.

[60] M. Boll, G. Fuchs, C. Meier, A.X. Trautwein, A. El Kasmi, S.W. Ragsdale, G. Buchanan, D.J. Lowe, Redox centers of 4-hydroxybenzoyl-CoA reductase, a member of the xanthine oxidase family of molybdenum-containing enzymes, J. Biol. Chem. 276 (2001) 47853–47862.

[61] R. Hille, Molybdenum and tungsten in biology, Trends Biochem. Sci. 27 (2002) 360–367.

[62] H. Schindelin, C. Kisker, K.V. Rajagopalan, Molybdopterin from molybdenum and tungsten enzymes, Adv. Protein Chem. 58 (2001) 47–94.

[63] D.J. Lowe, Enzymes of the xanthine oxidase family: the role of molybdenum, Met. Ions Biol. Syst. 39 (2002) 455–479.

[64] J. Gibson, M. Dispensa, C.S. Harwood, 4-Hydroxybenzoyl-CoA reductase (dehydroxylating) is required for anaerobic degradation of 4-hydroxybenzoate by *Rhodopseudomonas palustris* and shares features with molybdenum-containing hydroxylases, J. Bacteriol. 179 (1997) 634–642.

[65] H. Dobbek, L. Gremer, R. Kiefersauer, R. Huber, O. Meyer, Catalysis at a dinuclear [CuSMo(=O)OH] cluster in a CO dehydrogenase resolved at 1.1-A resolution, Proc. Natl. Acad. Sci. 99 (2002) 15971–15976.

[66] C. Enroth, B.T. Eger, K. Okamoto, T. Nishino, T. Nishini, E.F. Pai, Crystal structures of bovine milk xanthine dehydrogenase and xanthine oxidase: structure based mechanism of conversion, Proc. Natl. Acad. Sci. 97 (2000) 10723–10728.

[67] M.J. Romao, M. Archer, J.J. Moura, J. LeGall, R. Engh, M. Schneider, P. Hof, R. Huber, Aldehyde oxidoreductase activity in *Desulfovibrio gigas*: in vitro reconstitution of an electron-transfer chain from aldehydes to the production of molecular hydrogen, Science 270 (1995) 1170–1171.

[68] W. Reichenbecher, B. Schink, Towards the reaction mechanism of pyrogallol-phloroglucinol transhydroxylase of *Pelobacter acidigallici*, Biochim. Biophys. Acta 1430 (1999) 233–245.

[69] R.C. Bray, The inorganic biochemistry of molybdoenzymes, Q. Rev. Biophys. 21 (1988) 299–329.

[70] M.J. Barber, M.P. Coughlan, K.V. Rajagopalan, L.M. Siegel, Properties of the prosthetic groups of rabbit liver aldehyde oxidase: a comparison of molybdenum hydroxylase enzymes, Biochemistry 21 (1982) 3561–3568.

[71] B.A.S. Barata, J. LeGall, J.J. Moura, Aldehyde oxidoreductase activity in *Desulfovibrio gigas*: in vitro reconstitution of an electron-transfer chain from aldehydes to the production of molecular hydrogen, Biochemistry 32 (1993) 11559–11568.

[72] R.K. Thauer, J. Jungermann, K. Decker, Energy conservation in chemotrophic anaerobic bacteria, Bacteriol. Rev. 41 (1977) 100–180.